AMORPHOUS SIC: APPLICATIONS FOR SILICON SOLAR CELLS

S. Janz, S. Reber, S. W. Glunz
Fraunhofer Institute for Solar Energy Systems ISE, Heidenhofstr. 2, D-79110 Freiburg,
Corresponding author: Stefan Janz, Tel.: +49-761-4588-5247, Fax.: +49-761-4588-9250,
E-mail: stefan.janz@ise.fraunhofer.de

ABSTRACT: In this publication we give an overview of the activities at Fraunhofer ISE investigating SiC as an alternative to SiN_x and SiO_x. Our first aim was to create a conductive diffusion barrier for our Recrystallized Wafer Equivalent (RexWE). Parameters and characteristics as etch resistance, annealing behaviour (stress development, effusion of hydrogen and dopants), bandgap tuning, p- and n-doping (influence on resistivity) and diffusion behaviour were investigated. Especially the good thermal stability of our layers let us start to optimize Si_xC_{1-x} as a rear-side surface passivation on p-type silicon. On a PERC structure an open-circuit voltage of 682 mV after firing at 800°C could be achieved. Further photovoltaic applications of this variable layer (single layer or stack) will be discussed.

Keywords: SiC, Thin Film, passivation

1 INTRODUCTION

Amorphous silicon based layers like SiN_x or SiO_x can be found in numerous Si solar cell applications. They are used as diffusion barriers, anti-reflection coatings, surface passivation layers or as a hydrogen source to passivate the silicon bulk material. The only handicaps if any are their relatively poor thermal stability and their lack of conductivity (electrical and thermal). Therefore we tried to establish SiC as a substitute with even better characteristics.

1.1 SiC layer deposition

All depositions were realized by plasma enhanced chemical vapour deposition (PECVD). The reactor (AK400M from Roth&Rau) had two different plasma sources working at 2.45 GHz (microwave) and 13.56 MHz (radio frequency). These two sources enabled us to influence, almost independently, deposition parameters like collision rate inside the plasma, growth rate and surface damage generation. The precursor gases silane (SiH_4) and methane (CH_4) for deposition, diborane (B_2H_6) and phosphine (PH_3) for doping, and H_2 and Ar for reasons like etching or plasma stabilization were used. Homogeneity and defect generation were mainly influenced by the process pressure varying from 5 to 30 Pa. With specially developed reactor adaptations, deposition temperatures up to 650°C could be applied.

2 PHYSICAL PROPERTIES OF SiC

2.1 Etching of SiC

The etch resistance of stoechiometric SiC is well known from literature. Best etching results are proposed with fluorine based processes. In our plasma reactor the maximum etching rate achieved was 30 nm/min with a NF_3/Ar gas mixture but higher rates with SF_6 (120 nm/min) were also reported [1]. The literature data for wet chemical etching are focused on c-SiC [2]. They report good etching results only with molten KOH (> 600°C). When transferring these experiments to wet chemical etching of a-SiC one could presume that, due to a higher defect density (hydrogen content) the etching rates should be much higher. We focused our investigations in the field of wet chemical etching on standard processes for photovoltaics. An exposure to KOH (>3%, 90°C) for >10 min, e.g., led to no etching effect at all. An annealed (950°C for 10 min) stoechiometric SiC layer of 300 nm thickness could even resist 85°C hot KOH (50%) for 30 min with almost no etching effect on the SiC layer surface.

2.2 Annealing behaviour

When starting to anneal SiC (deposited at 350°C) the first effect which can be observed (from 550°C on) is hydrogen effusion. Fourier transformed IR (FTIR) spectroscopy showed, that the C-H_n, Si-H_n and more complex hydrogen related bonds cracked with temperature, led to hydrogen effusion and new Si-C bonds were formed. This network re-organization caused an increase in layer density, which for its part, affected the layer performance significantly. Amongst other effects an improvement in etch resistance and a change in layer stress σ was observed. The stress values for SiC layers, deposited at 350°C, 550°C and annealed at 950°C, presented in Table 1 were measured. For this the curvature of a polished 4" silicon wafer with a SiC layer on one side was scanned by a laser beam. The comparison of the wafer curvatures showed in principle a change of stress from compressive to tensile with increasing temperature. Increasing the deposition temperature seemed to have a similar effect as a subsequent annealing of the SiC layer.

Table 1: Stress values of SiC layers deposited at 350°C and 550°C, and annealed afterwards at 950°C for 15 min in argon atmosphere.

SiC layer	350°C	350°C & 950°C	550°C	550°C & 950°C
stress [MPa]	-266	+523	+162	+742

At further temperature increase (≥950°C) a crystallization process of the SiC layer starts [3]. By means of X-ray diffraction (XRD) measurements we mainly found crystalline phases of SiC (4H, 6H and 3C). Complementary Raman measurements showed also very small amounts of carbon and silicon clusters. These results clearly show, that stoechiometric amorphous SiC

layers preferentially crystallize to SiC crystals rather than forming C- or Si-clusters. Investigations concerning the influence of annealing on change in doping concentration and electrical conductivity will be presented below.

2.3 Optical bandgap tuning

One important factor which affects especially the optical behaviour of our SiC layers is the silicon and carbon content. This enabled us to vary the optical band gap E_g of our layers from 2.0 to 2.4 eV (see Fig. 1) just by changing the $SiH_4/(SiH_4+CH_4)$ gas flow ratio. This band gap variation went hand in hand with a change in refractive index *n* from 3.6 to 2.3. Because all other process parameters except the methane flow were kept constant, a smooth tuning of the optical parameters during deposition could be realized (see chapter 3.3).

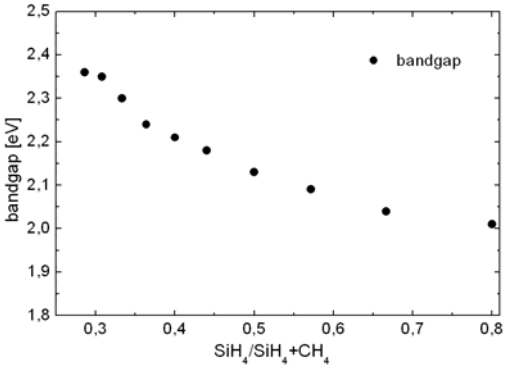

Fig. 1: Optical bandgap of SiC layers deposited with different $SiH_4/(SiH_4+CH_4)$ gas flow ratio.

2.4 Doping and conductivity

To increase the electrical conductivity, we doped our SiC layers with boron, phosphorous, and nitrogen by adding diborane, phosphine and nitrogen to the deposition gases. With secondary ion mass spectroscopy (SIMS) we determined boron concentrations from $4x10^{19}$ to $2x10^{20}$ cm^{-3} corresponding to 10 to 70 sccm of diborane flow during the SiC deposition process (highest measured phosphorous concentration $2x10^{20}$ cm^{-3} corresponding to 30 sccm of phosphine). Though the dopant concentration was very high, lateral conductivity measurements of the stoechiometric layers as deposited led to low conductivity of 10^{-11} Scm^{-1} ($5x10^{19}$ cm^{-3} of boron). An increase of the deposition temperature up to 650°C slightly changed the conductivity to 10^{-8} Scm^{-1}. Only after annealing the layers for 2 h at 650°C under vacuum conditions significantly enhanced the conductivity to 10^{-3} Scm^{-1}. This result fits very well to the hydrogen effusion theory, where free dangling bonds are generated, which can then be connected to the dopants and contribute thereby to the conductivity of the SiC layer.

Following the theory of Tauc *et al.* [4] we calculated band gap values E_g from optical transmission measurements. We deposited the doped layers on quartz glass substrates and measured them, as deposited or annealed, in a spectrophotometer, scanning from 400 to 1200 nm wavelength. The results are summarized in Table 2. Initially the band gap energies for differently doped layers as deposited are the same. They slightly decrease after an annealing at 500°C (2 h) and significantly change to values between 1.5 to 1.7 after annealing at 650°C (2 h). This effect can be explained by the activation of dopants with temperature as described above. An intermediate band state was generated, which broadened with the amount of free carriers and led to the observed band gap narrowing effect.

Table 2: Band gap values of differently doped stoechiometric SiC layers as deposited and annealed at 500°C and 650°C for 2 h under vacuum conditions.

	B_2H_6 20 sccm	B_2H_6 30 sccm	PH_3 40 sccm	N_2/H_2 0.02
as deposited	2.1	2.1	2.1	2.1
500°C	2.0	2.0		
650°C	1.7	1.6	1.7	1.5

2.5 Diffusion in SiC

The initially intended application for SiC at Fraunhofer ISE was an electrically conductive diffusion barrier layer in recrystallized Si thin-film solar cells. Especially transition metals, which significantly increase the minority carrier recombination rate in solar cells, had to be prevented from diffusing into the silicon bulk layer. With SIMS the change of implanted iron profiles with temperature was measured. By comparison with simulated data we calculated diffusion constants *D* for Fe (at 1200°C) of $3x10^{-15}$ to $4x10^{-16}$ cm^2/s for the stoechiometric SiC layers. This is, compared to values of other plasma deposited layers like SiO_2 ($7x10^{-13}$ cm^2/s) or SiN_x ($3x10^{-14}$ cm^2/s), an excellent value [5].

The second application was to use SiC as a source for hydrogen and dopants. Especially the hydrogen effusion was a most interesting topic when considering the bulk passivation effect in multicrystalline silicon solar cell material. Two different mechanisms are possible: (1) the cracking of hydrogen related bonds and (2) the effusion of free hydrogen from the SiC layers. Comprehensive studies with FTIR spectroscopy showed that after several minutes at above 600°C still a significant amount of hydrogen related bonds could be detected. We still do not have data for the amount of free hydrogen in the SiC layers but this effusion effect should be much faster due to the higher mobility of free hydrogen (or molecule diffusion). These two different effects most probably enable SiC to act as a hydrogen source during fast processing (e.g. contact firing) as well as a sustainable source for longer high temperature processes (e.g. emitter formation).

2.6 Passivation of silicon surfaces

With the quasi steady state photo conductance (QSSPC) method excellent lifetimes of >1500 µs on Si_xC_{1-x} passivated 4" FZ wafers [6] could be measured. Because the carbon content of this layer was comparatively low, the passivation effect should be related to that of amorphous silicon (saturation of free bonds). Additional phosphorus doping further enhanced the passivation of our layers. This effect possibly came from fixed charges in the layer (field effect passivation). Another processing benefit was the surface cleaning before deposition by plasma etching (no additional wet-chemical cleaning) which could be realized in-situ. The carrier density imaging (CDI/ILM) [7] measurements in Fig. 2 show two 4" FZ wafers etched and coated with Si_xC_{1-x} in the same run. The results prove the excellent homogeneity of the etching and the deposition process on an area of 200x100 mm^2. The small areas with lower

lifetimes (black spots) could be explained with contaminations coming from tweezers prints or sometimes occurring blistering during deposition.

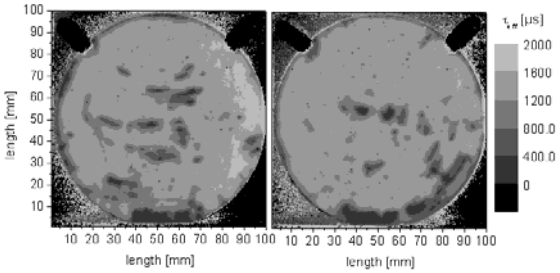

Fig. 2: CDI/ILM images of two passivated 4" FZ wafers processed in one run.

3 APPLICATIONS FOR PHOTOVOLTAICS

3.1 Recrystallized Wafer Equivalent (RexWE)

First solar cells with a standard contact structure (rear- and front-side) on recrystallized wafer equivalents could be realized. This was only possible with SiC diffusion barrier layers which were sufficiently electrical conductive [8]. Conductivity measurements of the wafer equivalent layer stack (SiC layer and cost-efficient RBSiC ceramic substrate) brought a specific resistivity for the boron doped SiC layer of ρ_{SiC}=18 Ωcm after RexWE processing. In comparison with the results in chapter 2.4 (10^{-3} Scm^{-1}→1000 Ωcm) the higher temperatures during RexWE processing seemed to further decrease the resistivity.

Table 3: Solar cell results on RexWE measured when contacting the cell base (p) from front- and rear-side

contact emitter/ base	V_{oc} [mV]	J_{sc} [mA]	FF [%]	η [%]
front-front	525	20.6	67	7.2
front-rear	524	20.5	67	7.1

A comparison of solar cell results on 1 cm^2 (base contact on front-side or rear-side) proved (see Table 3), that the series resistance of diffusion barrier layer and ceramic substrate did not limit the cell performance (identical fill factors). Though the solar cell results on highly impure substrates are not satisfying yet (due to cell processing problems [9]), maximum V_{oc} of 545 mV shows the good diffusion barrier performance of the SiC layer.

3.2 Passivation layer for solar cells

After the successful development of a highly passivating Si_xC_{1-x} layer, different layer systems based on different compositions were used for the rear passivation of solar cells with a high-efficiency front structure (oxide-passivated 120 Ω/sq emitter and evaporated front contacts). Again, not only the deposition but also the surface conditioning was performed in the PECVD reactor. E-gun evaporation was used for the deposition of the 2 µm thick Al layer and the laser-fired contacts (LFC) process was applied. First solar cell results with single passivation layers showed that not necessarily Si_xC_{1-x} layers, which led to excellent lifetimes when measuring with QSSPC, resulted in the best solar cell results. One possible explanation was a shunting effect of the aluminium contacts between passivation layer and silicon bulk. Nevertheless, efficiencies higher than 20% could be achieved [10].

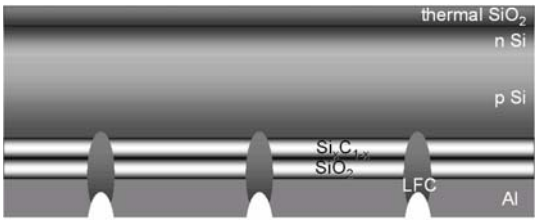

Fig. 3: PERC/LFC structure for annealing tests of rear-side passivation layers.

To investigate the influence of thermal annealing on passivation effectiveness we had to adapt our solar cell structure. Because of the introduced firing step two important factors had to be considered: (1) we could not use any metal on our cell structure during annealing and (2) the front-side had to be untextured. The metal would potentially destroy the passivation layer contaminate the bulk and cause massive recombination. A possible deterioration of the passivating thermal oxide at the pyramid tips (hot peaks) was the reason for dropping the texturization. Without any grid we had to measure with QSSPC and calculate V_{oc} from this data. The front-side passivation (thermal oxide) was assumed to be a better passivation layer than the rear-side one. Therefore the measured V_{oc} values should be limited by the passivation performance of the Si_xC_{1-x} layer. To be sure no blistering effect would disturbe our experiment, the Si_xC_{1-x} layer was capped with a PECVD SiO_2 layer.

The Si_xC_{1-x} layers used for this experiment were based on the excellent phosphorus doped passivation layers presented in chapter 2.6. The carbon content of these layers was varied to see if the temperature stability of the passivation performance was dependent on it. The firing of the cell structures was done in the furnace usually used for firing of screen printed front contacts. Because absorption conditions were much better than that of a standard cell structure, where the rear side is covered with aluminium, we reduced the temperature to 800°C which relates to a standard firing temperature of 880°C. In general it was striking that all passivation layers improved in performance with the firing step (see Table 4). Because the cell structure had already been annealed before the firing that effect had to be explained in connection with the Si_xC_{1-x} passivation layer. One possible reason could be an enhancement of the saturation effect due to lattice adaptation. Additional hydrogen effusing from the Si_xC_{1-x} bulk to the interface would be a second one. A third possible explanation could be the enhanced activation of the phosphorous atoms in the layer which would result in a stronger field effect.

Table 4: V_{oc} values calculated from QSSPC measurements on PERC structures without texturization before and after firing.

carbon content	V_{oc} before firing [mV]	V_{oc} after firing [mV]
Low	620	630
High	635	682

The fired cell structures were subsequently processed to solar cells. To finish the cell structure front- and rear-side (laser fired contacts) metallization had to be done. Solar cell results (0.5 Ωcm FZ substrate) can be found in Table 5.

Table 5: Solar cell results of fired PERC structures without texturization

carbon content	V_{oc} [mV]	J_{sc} [mA]	FF [%]	η [%]
Low	644	32.7	81	17.1
High	643	32.0	78	16.1

The V_{oc} were all limited to around 640 mV (almost independent from carbon content). The cell passivated with a Si_xC_{1-x} layer with low carbon content had even a better V_{oc} than calculated from the QSSPC measurement. We suppose these results come from still not fully understood effects related to the LFC contact formation.

3.3 Multilayer applications

The combination of SiC/Si_xC_{1-x} layers with different properties would be the next step for SiC layer applications in photovoltaics. Several ideas will be discussed in the following:

Alternative solar cell processes [11] could be realized, when using a stoechiometric SiC layer as a etch stop layer (texturization), diffusion barrier (emitter formation) and optical back reflector (n=2.4) in combination with the temperature stable Si_xC_{1-x} passivation layer.

Another possibility would be a Rugate filter, which is an optical coating [12] in which the refractive index varies sinusoidal throughout its thickness. It reflects light over a certain band of wavelengths and is considered to be one of the more complex applications of inhomogeneous optical coatings.

SiC quantum dot super lattices [13], which can be realized by combining stoechiometric and silicon rich Si_xC_{1-x} layer. The formation of the Si quantum dots is achieved through thermal annealing. Due to the flat quantum well of SiC compared to SiN_x and SiO_2 and the promising doping results a transport of the minority carriers generated in this layers could be possible.

Anti-reflection coatings of module glasses [14], which act as wear and etch resist upper layers, is also an obvious application. SiC should withstand the environmental influences quite well.

4 CONCLUSIONS AND OUTLOOK

The results presented in this publication were helpful to increase the basic understanding of SiC layers. Our layers could be successfully used as conductive diffusion barrier and excellent surface passivation layers. There are numerous possible applications of PECVD deposited SiC which are partly already investigated by our or other groups around the world. This work showed that the material has in fact the potential to combine several features like: diffusion barrier performance, tunable bandgap, p- and n-doping, conductivity, source for hydrogen and dopants, surface passivation (p- and n-type), thermal stability, stress tuning and a relatively flat quantum well for a better carrier transport in quantum dot super lattices. With SiC multilayer stacks some of these features could even be combined.

5 ACKNOWLEDGEMENTS

The authors want to thank Roth&Rau (Wuestenbrand, Germany) for their support in developing the special AK400M plasma reactor. Many of the investigations could only be realized with the committed help of colleagues like S. Fernandez-Robledo, E. Pink, H. Habenicht, D. Suwito (general understanding problems of the SiC behaviour), T. Roth, S. Riepe, M. Hofmann (surface passivation) and H. Lautenschlager, M. Kwiatkowska, A. Leimenstoll, S. Seitz and F. Granek (solar cell processing) and M. Vetter and his team at UPC (Barcelona, Spain) for the conductivity measurements.

Parts of this work were supported by the European Commission (EC) under contract no. SES6-CT-2003-502583 (Crystal Clear) and the Federal Ministry for the Environment, Nature Conservation and Nuclear Safety (BMU) under contract no. 0329850G (HERKULES-B).

6 REFERENCES

[1] U. Schmid, M. Eickhoff, Ch. Richter, G. Krötz, D. Schmitt-Landsiedel, "Etching Characteristics and Mechanical Properties of a-SiC:H Thin Films", Sensors and Actuators A 94 (2001), p. 87.

[2] D. Zhuang, J.H. Edgar, „Wet Etching of GaN, AlN and SiC: a review", Materials Science and Engeneering R48 (2005), p. 1-46.

[3] S. Janz, S. Reber, F. Lutz, C. Schetter, "SiC as an intermediate layer for CSiTF Solar Cells on Various Substrates", Proceedings of the 20th EUPVSEC, Barcelona (2005), p. 1016.

[4] J. Tauc, A. Menth, "States in the Gap", Journal of Non-Crystalline Solids (1972), p. 569.

[5] S. Reber, "Electrical Confinement for the Crystalline Silicon Thin-Film Solar Cell on Foreign Substrate", ibidem-Verlag Stuttgart (2000), ISBN: 3-89821-050-2.

[6] S. Janz, S. Riepe, M. Hofmann, S. Reber, S. Glunz, „Phosphorus-Doped SiC as an excellent p-type Si Surface Passivation Layer", Appl. Phys. Letters 88, 133516 (2006).

[7] J. Isenberg, S. Riepe, W.Warta, J. Appl. Phys., 93 (7), (2003), p. 4268.

[8] S. Janz, S. Reber, H. Habenicht, H. Lautenschlager. C. Schetter, "Processing of c-Si Thin-Film Solar Cells on Ceramic Substrate with Conductive SiC Diffusion Barrier Layer", Proceedings of the 4th WCPEC, Hawaii (2006), in print.

[9] S. Janz, S. Reber, H. Habenicht, H. Lautenschlager. C. Schetter, F. Lutz "Solar Cell Processing of Recrystallized Wafer Equivalent on Low-Cost Ceramics", this conference.

[10] S. W. Glunz, A. Grohe, M. Hermle, M. Hofmann, S. Janz, T. Roth, O. Schultz, M. Vetter, I. Martin, R. Ferré, S. Bermejo, W. Wolke, W. Warta, R. Preu, and G. Willeke, Proceedings of the 20th EUPVSEC, Barcelona (2005), p. 572.

[11] S. W. Glunz, S. Janz, M. Hofmann, T. Roth, G. Willeke, "Surface Passivation of Silicon Solar Cells using Amorphous Silicon Carbide Layers", Proceedings of the 4th WCPEC, Hawaii (2006), in print.

[12] R. M. Young, W. D. Partlow, "Amorphous silicon, amorphous carbon and amorphous silicon carbide deposited by remote plasma chemical vapor deposition", Thin Solid Films, 213 (1992), p. 170.

[13] M. A. Green, "Third Generation Photovoltaics: Theoretical and Experimental Progress", Proceedings of the 19th EUPVSEC, Paris (2004), p. 3.

[14] M. Neander, F. Gromball, D. Neumann, N. Harder, W. A. Nositschka, "Anti-Reflection-Coating for Higher Solar Module Voltage", Proceedings of the 4th WCPEC, Hawaii (2006), in print.